2017

Extending the Upper Temperature Range of Microchip Gas Chromatography Using a Heater/Clamp Assembly

Abhijit Ghosh
Brigham Young University

Jacob E. Johnson
Brigham Young University

Johnathan G. Nuss
Brigham Young University

Brittany A. Stark
Brigham Young University

Aaron R. Hawkins
Brigham Young University

See next page for additional authors

Original Publication Citation

Ghosh, A., Johnson, J. E., Nuss, J. G., Stark, B. A., Hawkins, A. R., Tolley, L. T., Iverson, B. D., Tolley, H. D., and Lee, M. L. (2017). Extending the upper temperature range of gas chromatography with all-silicon microchip colwnns using a heater/clamp assembly. Journal of Chromatography A, 151 7, 134-141.

Extending the Upper Temperature Range of Microchip Gas Chromatography Using a Heater/Clamp Assembly

Abhijit Ghosh[a], Jacob E. Johnson[b], Johnathan G. Nuss[b], Brittany A. Stark[b], Aaron R. Hawkins[b], Luke T. Tolley[a], Brian D. Iverson[c], H. Dennis Tolley[d] and Milton L. Lee[a]*

[a] Department of Chemistry and Biochemistry, Brigham Young University, Provo, UT 84602 USA

[b] Department of Computer and Electrical Engineering, Brigham Young University, Provo, UT 84602 USA

[c] Department of Mechanical Engineering, Brigham Young University, Provo, UT 84602 USA

[d] Department of Statistics, Brigham Young University, Provo, UT 84602 USA

Abstract

Miniaturization of gas chromatography (GC) instrumentation is of interest because it addresses current and future issues relating to compactness, portability and field application. While incremental advancements continue to be reported in microchip GC, the current performance is far from acceptable. This lower performance compared to conventional GC is due to factors such as pooling of the stationary phase in corners of non-cylindrical channels, adsorption of sensitive compounds on incompletely deactivated surfaces, shorter column lengths and less than optimum interfacing to injector and detector. In this work, a microchip GC system was developed that solves the latter challenge, i.e., microchip interfacing to injector and detector. A microchip compression clamp was constructed that seals injector and detector fused silica interface tubing to inlet and outlet ports of the microchip channels with minimum extra-column dead volume, and that allows routine operation at least up to 300 ºC. The compression clamp was constructed of a low expansion alloy, Kovar™, to minimize leaking due to thermal expansion

mismatch at the interface during repeated thermal cycling. A 5.9 m channel with a cross-section that approximately matches a 100 μm i.d. cylindrical fused silica column was fabricated in a silicon wafer using wafer bonding and deep reactive ion etching (DRIE) and coated statically with a 1% vinyl, 5% phenyl, 94% methylpolysiloxane stationary phase. High temperature separations of C10-C40 *n*-alkanes and a commercial diesel sample were demonstrated using the system under both temperature programmed GC (TPGC) and thermal gradient GC (TGGC) conditions. TGGC analysis of a complex essential oil sample was also demonstrated.

Keywords

High temperature

Microchip

Gas chromatography

Semi-volatile compounds

Thermal gradient

1. Introduction

Since the introduction of the first microfabricated gas chromatograph (i.e., microchip GC) by Terry *et al*. in 1979 [1], a variety of micromachining techniques have been employed to generate miniature GC columns [2-5]. Unfortunately, the performance of microchip GC remains inferior to conventional GC. Columns for microchip GC are fabricated in substrates such as silicon [6], glass [7], ceramic [8], polymer [9] and metal [10]. Depending on the nature of the fabrication process, microcolumns fabricated in silicon (the most popular substrate) can be rectangular (dry etched) or trapezoidal (wet etched) in cross section. Interestingly, Golay [11]

predicted the performance of rectangular columns to be superior to circular columns. However, the theoretical advantages of rectangular microcolumns are usually compromised in practice because of limited length, surface texture/adsorption, difficulties encountered in interfacing and poor coating efficiency.

In conventional GC, 15 to 30 m capillary columns are employed for most analyses. In contrast, the majority of microfabricated columns fall within the range of 0.5-6 m in length. Some examples include a 0.9 m column fabricated by Kolesar and Reston [3], a 1 m column reported by Noh *et al.*[4], 1.5-3.0 m columns micromachined by Terry *et al.*[1], a 3 m column reported by Lambertus *et al.*[5], a 5.6 m spiral column reported by Yu *et al.*[2], a MEMS-based 6 m column used by Sun *et al.*[12] for the analysis of benzene and toluene mixtures, a 6 m primary column and 0.5 m secondary column for microfabricated GCxGC reported by Serrano *et al.*[13], and a 7.5 m primary microcolumn fabricated in glass that was used for GCxGC separation of BTEX by Lewis *et al.*[7].

In addition to the limitation of microfabricated column length, various lithographic processes used for their fabrication can expose surface active sites (i.e., reactive functional groups and trace impurities) present in the substrates that can affect chromatographic performance adversely. Fortunately, the most common substrate, silicon, is generally near 100% pure silicon, but can contain ppb levels of boron, phosphorus, arsenic, or antimony as dopants. In contrast, commonly used borosilicate glass, Pyrex, contains approximately 80% silica (SiO_2), 12% boric oxide (B_2O_3), 4% sodium oxide (Na_2O), 2% alumina (Al_2O_3), and traces of iron oxide (Fe_2O_3), calcium oxide (CaO), magnesium oxide (MgO) and chlorine (Cl). Ceramic substrates can contain a variety of oxides, nitrides and carbides.

To date, capillary tubing has typically been used to introduce and purge solutions during microchip channel pretreatment and coating of the stationary phase, and to connect the injector and detector to the microchip. The simplest approach has been to attach these capillary transfer lines to the microchip using an adhesive that has a thermal coefficient of expansion that is similar to that of the microchip [5, 6]. Another approach has been the use of Nanoport™ assemblies with epoxy [14]. While simple in concept, finding an ideal adhesive that has a desirable thermal coefficient of expansion and that can withstand high operating temperatures is not trivial. Epoxies, which are the most popular adhesives used for attachment of microfluidic ports, have significantly different thermal expansion coefficients than silicon [15]. Mismatching of thermal expansion coefficients causes delamination of the adhesive and subsequent leakage at the interface when subjected to thermal cycling. Furthermore, interfacing with most epoxy adhesives is difficult, leading to a high rate of failure. For example, during the curing process, the epoxy becomes less viscous at elevated temperature, and can be drawn into the channel by capillary action, oftentimes clogging the 50-70 μm deep microchannels. Another major limitation imposed by adhesive attachment of the interface capillaries is the upper operational temperature [16]. In GC, the analysis of semi-volatile compounds, such as polycyclic aromatic hydrocarbons (PAHs) and petroleum products, requires temperatures approaching and even surpassing 300 ºC. Unfortunately, very few commercially available adhesives can operate at such high temperatures. The commonly used Hysol® epoxy is good to around 200 ºC, limiting its application range to volatile compounds. Duralco™ 133, a thermally conductive adhesive, is rated to 315 ºC; however, it often showed leakage after several temperature cycles. Epoxies that have low thermal expansion did not provide a proper seal.

The only report to date describing high temperature microchip GC utilized a stainless-steel manifold with special fittings and ferrules to connect the capillary leads to the inlet and outlet of the microchip. With this design, the authors were able to operate up to 350 ºC. This allowed the analysis of semi-volatile compounds such as specified in ASTM 2887 and EPA 8310 using microchip GC [17].

Deactivating and coating microchip channels present their own unique challenges. In particular, static coating of microchip columns is more challenging than open tubular columns due to more frequent occurrence of air bubbles and plugging [18]. Since microchip channels are often non-cylindrical with abrupt bends (i.e., right angle or serpentine), non-homogeneous accumulation of liquid stationary phase in areas of increased curvature, such as in corners, is often experienced [19]. This compromises chromatographic efficiency and peak symmetry. Microfabrication of channels in silicon or glass leads to smooth channel surfaces, which is prerequisite for efficient static coating. In contrast, channels fabricated in ceramic substrates are oftentimes rough and porous, which leads to lower performance.

Thermal gradient gas chromatography (TGGC), which was originally introduced by Zhukhovitskii in the 1950s [20] and studied by various groups [21-23] since then, can inherently correct for some of the compromised chromatographic performance of non-ideal columns/channels by imposing a negative temperature gradient along the column length. While there have been varied opinions [24-26] concerning the value of this chromatographic mode, Blumberg recently reported [27] that focusing can help recover losses in resolution and speed resulting from non-ideal chromatographic conditions. Recently, we showed [16] that by applying a thermal gradient on a 1.4 m microchip GC column, peak tailing was significantly reduced, narrow chromatographic bands were obtained, and detector signal-to-noise ratio was increased.

Navaei *et al.* [28] used a series of concentric heaters on a 3 m spiral silicon microcolumn to generate a temperature gradient. A 30 ºC gradient was shown to focus three hydrocarbons under investigation. TGGC is expected to be particularly effective for short columns, typical of microchip columns. Applying a negative temperature gradient on a long column is cumbersome and complex. Several studies [20-28] explored theoretical and practical aspects of negative thermal gradients. Recently, with a 1.8 m open tubular capillary column, Boeker and Leppert [29] were able to generate remarkably fast, high temperature separations with very narrow peaks, thereby, reasserting the value of negative gradients in GC.

In the work [29] by Boeker and Leppert, temperatures up to 320 ºC were reported using a resistively heated metal capillary column. The use of epoxy for connecting leads to the microchip column in our previous work [16] limited the temperature to 180 ºC. A 3 m column fabricated by Navaei *et al.* [28] used epoxy assisted Nanoport™ fittings for interfacing, which restricted operation to relatively low temperatures.

In this paper, we report a novel microchip GC design that was operated up to 375 ºC. A fixture made from low thermal expansion material housed a cartridge heater for applying heat to the microchip, and provided simple and effective attachment of the inlet and outlet leads. While conventional temperature programming (TPGC) could be utilized with this device, a gradient along the microchip could also be generated by employing an insulating polyimide foam layer and convective airflow. In this work, we demonstrate several high temperature TGGC separations, which to our knowledge represent the highest operating temperatures reported to date for microchip GC.

2. Experimental

139 *2.1 Reagents and standards*

140 Silicon wafers (100 mm in diameter, 500 μm thick), were purchased from Nova
141 Electronic Materials (Flower Mound, TX, USA); spectrophotometric grade *n*-pentane was
142 purchased from Alfa Aesar (Ward Hill, MA, USA); dicumyl peroxide was purchased from
143 Sigma–Aldrich (St. Louis, MO, USA) and a 1% vinyl, 5% phenyl, 94% methylpolysiloxane (SE-
144 54, catalog no. 21106) was purchased from Supelco (Bellefonte, PA, USA). A performance test
145 mixture (31678) containing 16 *n*-alkanes (C10-C40) was purchased from Restek (Bellefonte, PA,
146 USA); a diesel sample was obtained from a local Chevron gas station in Provo, UT, USA; and a
147 *ylang ylang* essential oil was obtained from Young Living Essential Oils (Lehi, UT, USA).

148 *2.2 Microchip fabrication*

149 Prior to cleanroom fabrication, 250 μm diameter through-holes were laser-drilled into a
150 500 μm thick, 10.16 cm diameter silicon wafer to form the inlet and outlet access holes to the
151 column. The wafer surface was then re-polished using a chemical-mechanical polisher to restore
152 a smooth, particle-free surface. After polishing, the wafer was dehydrated by heating to 150 ºC
153 for 20 min. The serpentine channel represented in Figure 1A was then patterned onto the wafer
154 using AZ 3330 photoresist and AZ 300K developer (AZ Electronic Materials, Branchburg, NJ,
155 USA). After patterning, the photoresist was baked at 130 ºC for 120 min to harden the mask. The
156 exposed silicon was then dry-etched in an STS Multiplex ICP Etcher (Imperial Park, Newport,
157 UK), which resulted in the formation of the rectangular channel profile shown in Figure 1B.

158 After etching the channel, the photoresist mask was removed by submersing the wafer in
159 Nano-Strip (Cyantek, Fremont, CA, USA) at 90 ºC for 12 h. Next, a uniform layer of silicon
160 dioxide with a thickness of 330 nm was grown on the surface of the etched wafer, as well as on a
161 new (i.e., without features) polished silicon wafer, in an oxidation furnace heated to 1100 ºC.

The two wafers were then thoroughly cleaned and rinsed with isopropanol and deionized water, brought into contact with each other and placed in an oxidation furnace, which was slowly heated from 140 ºC to 1100 ºC at a rate of 2 ºC/min. The furnace was held at 1100 ºC for 3 h, and then cooled to 500 ºC at a rate of -2 ºC/min. This resulted in fusion of the two oxide layers, creating a sealed column channel with cross-section of 158 μm x 80 μm as shown in Figure 1C. After bonding, the sealed wafer was diced into a single 6.35 cm x 6.35 cm square so that the inlet and outlet holes were located near one edge of the microchip. The length of the microcolumn was measured to be 5.9 m in length.

2.3 Microchip manifold/heater clamp

A manifold for holding the silicon microchip was fabricated, and consisted of top and bottom sections (Figure 2A). It was designed to be clamped onto the microchip with one side providing sealing to the inlet and outlet holes in the microchip. The microchip was fabricated with two alignment holes located on either side of the inlet and outlet openings. These holes helped in precise alignment of the inlet and outlet of the microchip with the manifold. A polyimide film was used as a gasket to provide a leak-free seal between the microchip holder (manifold) and the silicon microchip. High temperature ferrules (FS.25-5, Valco, Houston, TX, USA,) with operating temperature up to 350 ºC were used to connect 100 μm i.d. x 236 μm o.d. fused silica capillary tubing leads (Polymicro Technologies, Phoenix, AZ, USA) to the microchip holder. The capillary tubing provided convenient access to coat the channels of the microchip as well as connections to the GC injection port and detector. For final assembly, the microchip was positioned between the two sections of the microchip holder. The two alignment pins on the microchip holder were inserted into the alignment holes on the microchip for proper positioning of the microchip in the device. The polyimide film also had alignment holes that

matched those on the microchip. When the microchip was inserted into the microchip holder, the alignment pins were inserted through the polyimide film and into the microchip. The microchip was held in place while tightening two screws to clamp the assembly together. The screws were tightened in steps with equal pressure applied during each step. The pressure was measured (17 N cm) using a torque screwdriver (Seekonk, MA, USA). After assembly (Figures 2B and 2C), the microchip and microchip holder were placed inside a GC oven and heated to 300 ºC overnight. The heating step resulted in softening of the polyimide film, which allowed the film to soften and fill into any flaws in the sealing surfaces of the microchip and microchip holder. The microchip holder had holes to accommodate a cartridge heater (25 W) and sensors. The heater and sensors were used for heating and temperature control, respectively. Since heat was only applied to one edge of the microchip, heating of the microchip holder created a thermal gradient across the microchip.

2.4 Microchip channel coating

As just described, the inlet and outlet ends of the microchannel were accessed with 100 µm i.d. x 236 µm o.d. silica capillaries. Ferrules were used to achieve proper sealing. The stationary phase solution contained 0.75% w/w 1% vinyl, 5% phenyl, 94% methylpolysiloxane (SE-54) and 1% dicumyl peroxide (used as crosslinking agent) in *n*-pentane. The coating solution was degassed briefly with sonication (Branson 1210, Danbury, CT, USA) before filling up the microchannel using a syringe pump (PHD 2000, Harvard Apparatus, Holliston, MA, USA). Once the channel was filled, the end of one capillary lead was sealed with both RTV sealant (732 multi-purpose sealant, Dow Corning, Midland, MI, USA) and silicone GC septum (part # 5183-4759, Agilent, Santa Clara, CA, USA).

One of the major problems with the static coating method is expansion of gas bubbles when vacuum is applied to evaporate the solvent.[30] Such bubbles usually originate from inefficient degassing of the coating solution and/or air trapped in the micro-cavities in the channel walls or at the capillary lead/microchip interfaces. Trapped air bubbles were effectively removed/dissolved by degassing, followed by pressurizing the solution inside the microchannel with 100 psi helium for 1 h. The open end of the microchip capillary lead was connected to a vacuum pump for static coating. During solvent evaporation, the microchip was submersed in a water bath at room temperature to ensure constant and uniform temperature. The column was maintained under vacuum for an additional half hour to ensure complete solvent evaporation. Curing of the stationary phase was performed by heating the microcolumn from 40 ºC to 250 ºC at 1 ºC/min and holding at 250 ºC overnight. The film thickness of the stationary phase was calculated to be 0.1 μm.

2.5 Instrument set-up for thermal gradient studies

A Perkin Elmer Clarus 600 gas chromatograph equipped with split/splitless injector and flame ionization detector (FID) (PerkinElmer, Shelton, CT, USA) was used for GC analysis. The injector and detector were set at 250 ºC. The capillary leads to the inlet and outlet of the microchip were connected to the injector and detector of the GC and heated to 285 ºC using double glass-insulated resistance wire (Pelican Wire Company, Naples, FL, USA). An in-house LabVIEW program (National Instruments, Austin, TX, USA) was integrated with an Arduino Uno microcontroller (www.arduino.cc) for temperature control by pulse-width modulation (PWM). Monitoring of the gradient across the microchip and the transfer lines was accomplished by positioning thermocouple probes at specific locations.

3. Results and discussion

3.1 Microchip holder design and use

A major impediment for high temperature semi-volatile compound analysis using microchip GC has been the limited temperature stability of connections from the microchip to injector and detector. Once fabricated, the microchip is connected to capillary leads for coating of the stationary phase and for interfacing to the GC system. It has been most common to use epoxies to connect the fused silica capillary leads to the microchip. This approach often results in immediate failure because the epoxy can run into and clog the column. In addition, adhesives usually limit the analytical application range because many adhesives do not operate at the desired upper temperature [16]. Another problem with using adhesives for column connections in microchip GC technology is mismatch of the coefficients of thermal expansion (CTE) between the adhesive and the microchip. It is not unusual for CTE values of common epoxies to be as high as 55 ppm/ºC while the CTE for silicon is 2.6 ppm/ºC at 20 ºC [15]. As the microchip is thermally cycled, differential expansion and contraction of the epoxy and silicon results in breakage of the seal and eventual leakage. In order to perform high temperature analysis, an alternative to the use of epoxies is required. In 2014, Gaddes *et al.*[17] introduced a stainless steel manifold that utilized ferrules instead of adhesives for connecting capillary tubing to the microchip. The microchip was housed inside the manifold and operated at temperatures up to 350 ºC inside a GC oven.

Since the microchip was clamped tightly in the microchip holder, as shown in Figure 2, it was important to choose appropriate materials with CTE values that matched the microchip as close as possible. Since large temperature changes occur during thermal cycling, choosing a material with a large mismatch in CTE would result in leakage and possible damage to the

253 microchip. For this reason Kovar™ (CRS Holdings, Wilmington, DE, USA), a nickel-cobalt-
254 ferrous alloy that has a low CTE value of 5.9 ppm/ºC similar to silicon (i.e., 2.6 ppm/ºC) and that
255 can withstand high temperatures, was chosen for the microchip holder. As a result, the column
256 assembly could be operated at temperatures as high as 375 ºC.
257 *3.2 Thermal gradient profile*
258 Prior to performing TGGC separation, the shapes of the gradient at different temperatures
259 were studied with a silicon wafer of similar dimensions and thickness (without channels) as the
260 microchip used in this study. A 6.35 cm x 6.35 cm square silicon microchip (1 mm thick) was
261 held at one end between two aluminum blocks. The aluminum blocks housed two 150 W
262 cartridge heaters to heat the microchip from one end. A 12 V squirrel cage DC air blower
263 (Sparkfun, Boulder, CO, USA) was used for cooling the other end of the microchip.
264 Thermocouples (K type) and an IR camera (FLIR, Wilsonville, OR, USA) were used to monitor
265 the gradient profile across the microchip. It is worth mentioning that due to the low infrared (IR)
266 emissivity of silicon, the IR camera could only indicate the shape and uniformity of the gradient,
267 but not the actual temperatures. For this reason, thermocouples were attached, using high
268 temperature polyimide tape, onto the microchip and heater to measure the actual temperatures.
269 Gradient shapes were observed for heater temperatures of 125 ºC, 250 ºC and 300 ºC with and
270 without the fan. Figure 3A shows the IR camera image of a gradient on the microchip when the
271 hot end (bright yellow) and cool end (green) temperatures were measured as 250 ºC and 50 ºC,
272 respectively, using thermocouples. The orange-red mark at the right bottom is due to the
273 polyimide tape used to attach a thermocouple to measure the end temperature. The dotted line
274 drawn in Figure 3A indicates where the temperature measurements were taken to construct the
275 plot in Figure 3B (temperature vs. distance from the heated end of the chip) using the IR camera

276 software. As noted previously, the temperature values obtained with the IR camera alone were
277 not accurate; rather, the temperature gradient represented in Figure 3B was used in conjunction
278 with the thermocouple temperature data at the heated and cooled ends to quantify the thermal
279 profile.

280 Because the shape of the gradient (slope) must be uniform across the microchip, the
281 gradients at various distances from the edge of the microchip were also recorded (Figure 3C). It
282 can be easily observed that the gradient profiles across the microchip were uniform with an
283 exponential shape. Such an exponential shape is desirable because a steep initial slope allows
284 strong focusing of the analytes, while progression to a shallower slope increases the resolution of
285 eluting compounds.

286 *3.3 Separation of n-alkanes*

287 A standard test mixture containing 50 µg/mL C10-C40 *n*-alkanes in *n*-hexane, was
288 separated using both TPGC and TGGC. The boiling points of the mixture components extended
289 from 174.1 ºC to 523.9 ºC. With the current TGGC heating arrangement, it was impossible to
290 elute the higher boiling compounds without setting the heater at an extremely high temperature.
291 This is due to the fact that because only one heater was used for generating the temperature
292 gradient across the microchip; the temperature at the end of the microchip, which controls
293 elution, was not hot enough to elute higher boiling point hydrocarbons. Even after setting the
294 heater temperature at 350 ºC, the end temperature of the microchip was 178 ºC. Using higher
295 temperatures for an extended period of time at the heater end is not feasible because of the
296 limited thermal stability of the stationary phase and the polyimide sealing film near the heater.
297 Therefore, the microchip was insulated with a polyimide foam (Solimide® foams, Magnolia,
298 AR, USA) enclosure to minimize heat loss across the microchip (Figure 4). The insulation made

a significant difference, as the end temperature was elevated to 230 ºC from 178 ºC for the same 350 ºC heater temperature.

The chromatogram in Figure 5A was obtained by initially setting the heater temperature at 70 ºC while air from the fan was delivered at the other end to generate a 30 ºC gradient across the microchip. Transfer lines connecting the microchip to the injector and detector of the GC were maintained at 285 ºC. Next, 1 µL of the *n*-alkane mixture was manually injected into the microchip with a 10:1 split ratio. Immediately after injection, the heater was ramped at a rate of 15 ºC/min up to 375 ºC. The final lower end temperature of the microchip was 275 ºC. To compare this TGGC analysis with TPGC, a similar temperature programming time window was used to separate the same hydrocarbon mixture. For TPGC, the microchip was housed inside the oven of the GC without any polyimide insulation, and 1 µL of the solution was manually injected with a 10:1 split ratio at 40 ºC oven temperature and ramped at a rate of 15 ºC/min up to 275 ºC (Figure 5B). The carrier gas velocity for both analyses was kept constant at 55 cm/s and an FID was used to record the chromatograms.

All 16 components were successfully separated using the 5.9 m long microcolumn using both temperature programming modes. Although, the analytes were added to the mixture in similar concentrations, boiling point discrimination from the split/splitless inlet was obvious for the higher molecular weight compounds using both TPGC and TGGC. C10 was much better separated from the solvent peak using TPGC. This is because the temperature at the end of the TGGC column could not reach 40 ºC at the beginning at the analysis. However, the overall resolution from TGGC was superior to that from TPGC, even though both used the same programming rate. From the enlarged image of the C30 peak in both chromatograms, it can be seen that TGGC gave more symmetrical peaks than TPGC. For TPGC, the oven was operated

from 40 ºC to 275 ºC and the whole microcolumn experienced uniform heating inside the GC oven. In contrast, stationary phase bleeding at the end of the TGGC chromatogram occurred because the front end of the microcolumn was elevated to 375 ºC to reach an elution temperature of 275 ºC at the end of the microchip, which was the maximum temperature that any portion of the TPGC column experienced.

In order to diminish stationary phase bleeding, a secondary heater was introduced in the heater/clamp assembly to provide uniform heat to the remainder of the microchip not attached to the heater/clamp. With this addition, the microchip end temperature could be raised to 275 ºC without the necessity of increasing the clamp heater temperature above 300 ºC where the stationary phase starts to bleed. A 7.5 cm x 7.5 cm square mica heater (HM 6962, Minco, Minneapolis, MN, USA) was attached to the underside of the microchip (indicated in Figure 4) with the help of a thin layer of thermally conductive paste (Arctic Silver 5, Arctic Silver®, Visalia, CA, USA). The mixture of *n*-alkanes was introduced with an initial gradient of 15 ºC (hot end set at 70 ºC and cool end at 55 ºC) and ramped at a rate of 15 ºC/min until the hot end reached 300 ºC. At this point, the cool end temperature was recorded as 190 ºC, and C24 eluted. The secondary heater temperature was increased gradually in increments of 10% over 20 min until the low end temperature reached 275 ºC. Figure 6 shows a chromatogram obtained using this dual heater arrangement for the C10-C40 *n*-alkane mixture. It is obvious that column bleed was greatly reduced.

In this chromatogram, however, solvent effects leading to split peaks are evident. When the dilute mixture of hydrocarbons in *n*-hexane was injected, flooding of the first section of the column led to splitting of the early peaks. As the column temperature increased and the solvent evaporated, this effect was eliminated for the less volatile sample components. This behavior is

well-known in the literature and can be corrected in future work [31]. Column overloading also is apparent for the last eluting compounds as the temperature profile along the column length approached isothermal conditions, and focusing of the band lessened.

3.4 Commercial diesel fuel separation

A commercial diesel fuel sample was obtained from a local Chevron station in Provo, UT, USA. Again, an initial 30 ºC gradient was established across the microchip with high and low temperatures of 70 ºC and 40 ºC, respectively. The transfer lines were kept at 275 ºC. A dilute sample of diesel fuel in *n*-pentane was injected into the microchip with 10:1 split. Helium carrier gas at a constant velocity of 55 cm/s, and an FID were used. After injection, the gradient was increased at a rate of 15 ºC/min up to 350 ºC and held constant. Figure 7 shows the resolution of diesel components up to C33.

3.5 Essential oil separation

For analyzing an *Ylang Ylang* essential oil sample, no insulation was used around the microchip. A gradient of 50 ºC was established at the time of injection with a heater temperature of 90 ºC and a microchip end temperature of 40 ºC. Injections were performed by quickly dipping the injection syringe needle in the neat oil and introducing it into the GC injection port using a split ratio of 10:1. The heater temperature was ramped at the rate of 5 ºC/min up to 250 ºC, and the transfer lines were maintained at 250 ºC. Figure 8 displays a typical chromatogram. Previous gas chromatographic analyses by researchers [32] have shown the presence of monoterpenes, sesquiterpenes, acetates, benzoates and phenols in *ylang ylang* oil. No effort was made to identify the peaks in the chromatogram; this separation was done only to demonstrate the ability of the microchip to resolve complex mixtures.

4. Conclusions

A microfluidic GC system was developed based on a new compression sealing technique. The system utilized a machined fixture made out of Kovar™, a low expansion nickel-cobalt-ferrous alloy, to minimize thermal expansion and subsequent leaking at the inlet and outlet ports of the microchannels during temperature cycling. This new laboratory system operated at temperatures up to 375 ºC, which is the highest temperature reported to this date for microfabricated gas chromatographic separations. The results of this study indicate that with proper implementation, TGGC can be successfully utilized to analyze complex volatile and semi-volatile compound mixtures and to enhance the separation performance of microchip gas chromatography.

References

[1] S.C. Terry, J.H. Jerman, J.B. Angell, Gas chromatographic air analyzer fabricated on a silicon wafer, IEEE T. Electron. Dev. 26(1979) 1880-6.

[2] M.L.C.M. Yu, J.C. Koo, P. Stratton, T. DeLima, and E. Behmeyer, A high performance hand-held gas chromatograph, Proc. ASME, Micro Electro Mechanical Systems, Anaheim, CA, Nov. 1998, 481–6.

[3] E.S. Kolesar, R.R. Reston, Review and summary of a silicon micromachined gas chromatography system, IEEE T. Compon. Pack. B 21(1998) 324-8.

[4] H.S. Noh, P.J. Hesketh, G.C. Frye-Mason, Parylene gas chromatographic column for rapid thermal cycling, J. Microelectromech. Syst. 11(2002) 718-25.

[5] G. Lambertus, A. Elstro, K. Sensenig, J. Potkay, M. Agah, S. Scheuering, et al., Design, fabrication, and microfabricated columns evaluation of for gas chromatography, Anal. Chem. 76(2004) 2629-37.

[6] G. Lambertus, R. Sacks, Stop-flow programmable selectivity with a dual-column ensemble of microfabricated etched silicon columns and air as carrier gas, Anal. Chem. 77(2005) 2078-84.

[7] J. Halliday, A.C. Lewis, J.F. Hamilton, C. Rhodes, K.D. Bartle, P. Homewood, et al., Lab-on-a-chip GC for environmental research, LCGC Eur. 23(2010) 514-23.

[8] E. Darko, K.B. Thurbide, G.C. Gerhardt, J. Michienzi, Characterization of low-temperature cofired ceramic tiles as platforms for gas chromatographic separations, Anal. Chem. 85(2013) 5376-81.

[9] A. Malainou, M.E. Vlachopoulou, R. Triantafyllopoulou, A. Tserepi, S. Chatzandroulis, The fabrication of a microcolumn for gas separation using poly(dimethylsiloxane) as the structural and functional material, J. Micromech. Microeng. 18(2008), 1-6.

[10] A. Bhushan, D. Yemane, J. Goettert, E.B. Overton, M.C. Murphy, Fabrication and testing of high aspect ratio metal micro-gas chromatograph columns, ASME 2004 International Mechanical Engineering Congress and Exposition, American Society of Mechanical Engineers 2004, 321-4.
[11] M.J.E. Golay, Theory of chromatography in open and coated tubular columns with round and rectangular cross-sections, Gas Chromatography: Butterworths, 1958, 36-55.
[12] J.H. Sun, D.F. Cui, Y.T. Li, L.L. Zhang, J. Chen, H. Li, et al., A high resolution MEMS based gas chromatography column for the analysis of benzene and toluene gaseous mixtures, Sensor Actuat, B: Chem. 141(2009) 431-5.
[13] G. Serrano, D. Paul, S.J. Kim, K. Kurabayashi, E.T. Zellers, Comprehensive two-dimensional gas chromatographic separations with a microfabricated thermal modulator, Anal. Chem. 84(2012) 6973-80.
[14] A.D. Radadia, A. Salehi-Khojin, R.I. Masel, M.A. Shannon, The effect of microcolumn geometry on the performance of micro-gas chromatography columns for chip scale gas analyzers, Sensor Actuat. B: Chem. 150(2010) 456-64.
[15] Coefficient of thermal expansion http://www.cleanroom.byu.edu/CTE_materials.phtml. (accessed 01.19.2017)
[16] A.Z. Wang, S. Hynynen, A.R. Hawkins, S.E. Tolley, H.D. Tolley, M.L. Lee, Axial thermal gradients in microchip gas chromatography, J. Chromatogr. A 1374(2014) 216-23.
[17] D. Gaddes, J. Westland, F.L. Dorman, S. Tadigadapa, Improved micromachined column design and fluidic interconnects for programmed high-temperature gas chromatography separations, J. Chromatogr. A 1349(2014) 96-104.
[18] S. Reidy, G. Lambertus, J. Reece, R. Sacks, High-performance, static-coated silicon microfabricated columns for gas chromatography, Anal. Chem. 78(2006) 2623-30.
[19] A. de Mello, On-chip chromatography: the last twenty years, Lab Chip, 2(2002) 48N-54N.
[20] A.A.Z. Zhukhovitskii, O.V. Sokolov, V.A., and Turkl'taub, N.M., A new method of chromatographic analysis, Doklady Akademii Nauk 77(1951) 435-8.
[21] R.E. Kaiser, Enriching volatile compounds by a temperature gradient tube, Anal. Chem. 45(1973) 965-7.
[22] W.A. Rubey, A different operational mode for addressing the general elution problem in rapid analysis gas chromatography, J. High Res. Chrom. 14(1991) 542-8.
[23] J.A. Contreras, A.Z. Wang, A.L. Rockwood, H.D. Tolley, M.L. Lee, Dynamic thermal gradient gas chromatography, J. Chromatogr. A 1302(2013) 143-51.
[24] R.W. Ohline, D.D. Deford, Chromathermography, the application of moving thermal gradients to gas liquid partition chromatography, Anal. Chem. 35(1963) 227-34.
[25] J.B. Phillips, V. Jain, On-column temperature programming in gas chromatography using temperature gradients along the capillary column, J. Chromatogr. Sci. 33(1995) 541-50.
[26] L.M. Blumberg, Limits of resolution and speed of analysis in linear chromatography with and without focusing, Chromatographia 39(1994) 719-28.
[27] L.M. Blumberg, Focusing cannot enhance resolution or speed limit of a GC column, J. Chromatogr. Sci. 35(1997) 451-4.
[28] M. Navaei, A. Mahdavifar, J.M.D. Dimandja, G. McMurray, P.J. Hesketh, All silicon micro-GC column temperature programming using axial heating, Micromachines 6(2015) 865-78.
[29] P. Boeker, J. Leppert, Flow field thermal gradient gas chromatography, Anal. Chem. 87(2015) 9033-41.

[30] C.F. Poole, The Essence of Chromatography, 1st ed.: Elsevier B.V. 2002, 79-170.
[31] K. Grob, Peak broadening or splitting caused by solvent flooding after splitless or cold on-column injection in capillary gas chromatography, J. Chromatogr. 213(1981) 3-14.
[32] E.M.R. Gaydou, R. Bianchini, J.P., Composition of the essential oil of ylang-ylang (Cananga-odorata hook fil. et thomson forma genuina) from Madagascar, J. Agr. Food Chem. 34(1986) 481-7.

Figure Legends

Figure 1. (A) Drawing of the serpentine pattern of the microcolumn; (B) drawing of a cross-section of the microcolumn; and (C) SEM images of actual microcolumn cross-sections.

Figure 2. (A) Drawing of the individual components of the microchip heating assembly; (B) drawing of the assembled heating manifold with microchip; and (C) photograph of the assembly illustrated in B.

Figure 3. (A) Thermal image of the temperature distribution on the microchip taken with an IR camera (the dotted line drawn on the image shows where data points were taken for construction of the profile in 3B); (B) shape of the thermal gradient along the dotted line drawn in Figure 3A; and (C) thermal gradients measured at four different locations across the microchip (right edge, approximately 0.5 cm from the right edge, center, and approximately 0.5 cm from the left edge).

Figure 4. Microchip heating assembly showing polyimide foam insulation and mica heater.

Figure 5. Chromatograms of semi-volatile *n*-alkanes (C10-C40) obtained using (A) TPGC and (B) TGGC.

Figure 6. Chromatogram of semi-volatile *n*-alkanes obtained using the dual heater TGGC assembly.

Figure 7. TGGC chromatogram of a commercial diesel sample.

Figure 8. TGGC chromatogram of *ylang ylang* essential oil.

Figure 1A, B, C

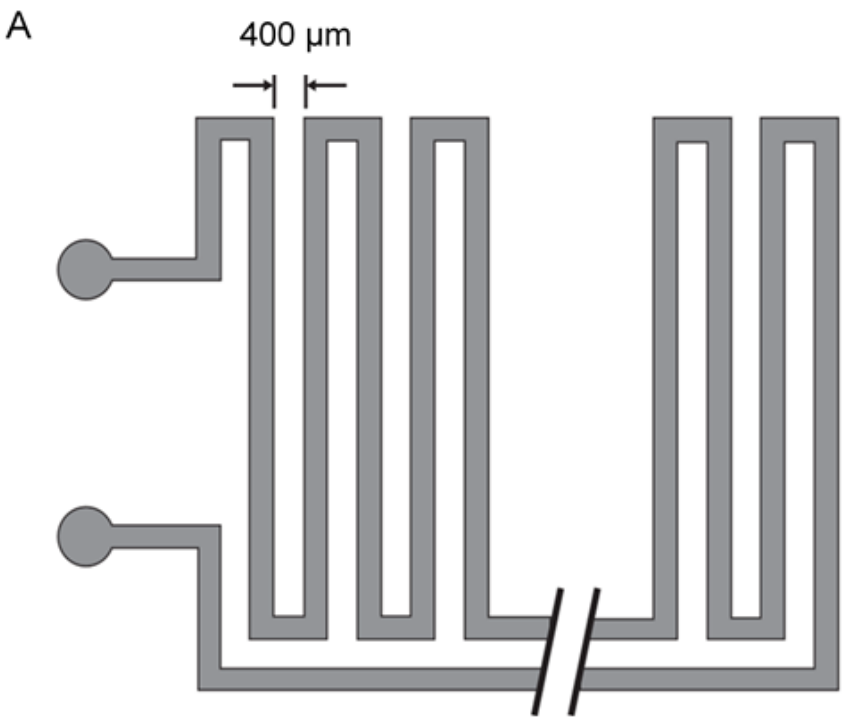

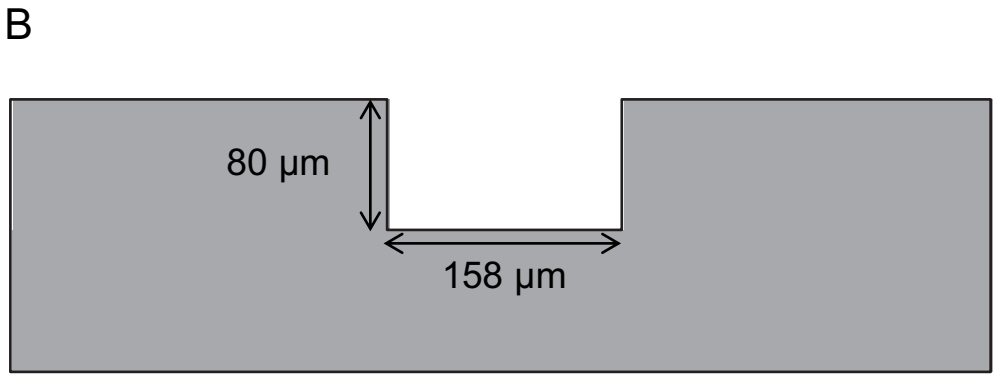

C

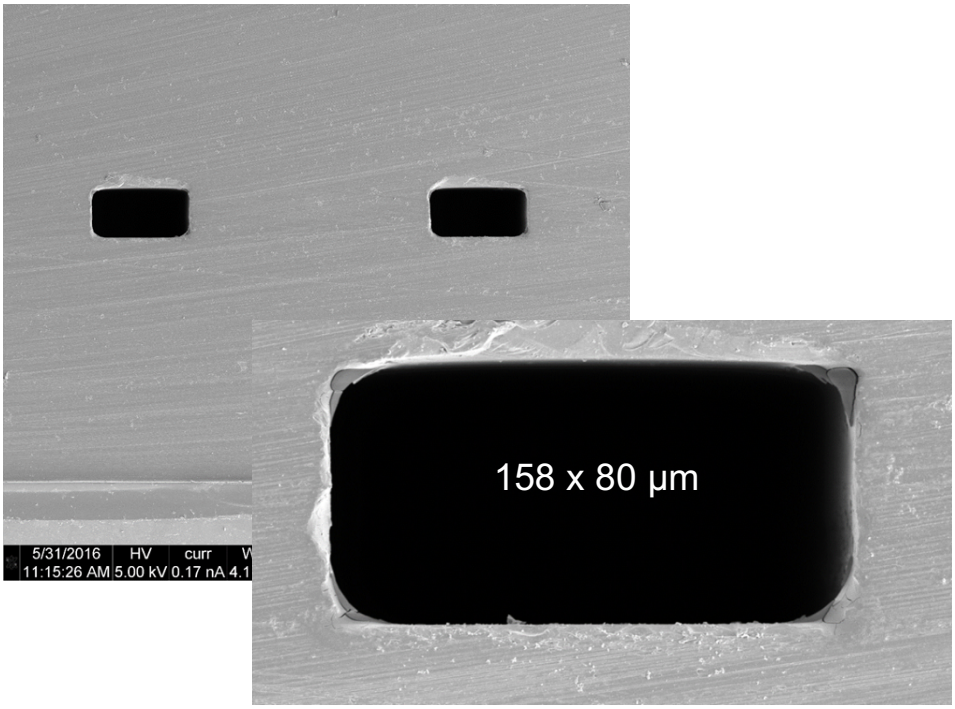

Figure 2A, B, C

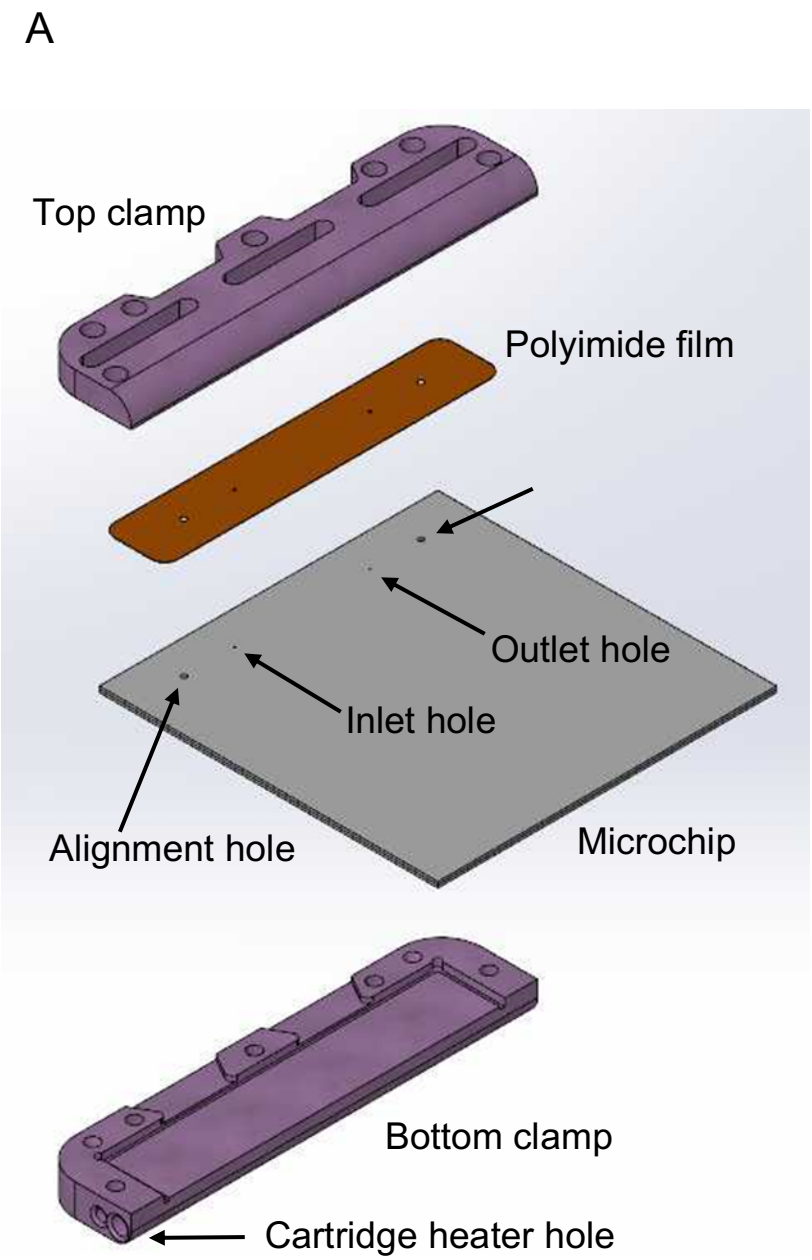
A
Top clamp
Polyimide film
Outlet hole
Inlet hole
Alignment hole
Microchip
Bottom clamp
Cartridge heater hole

B

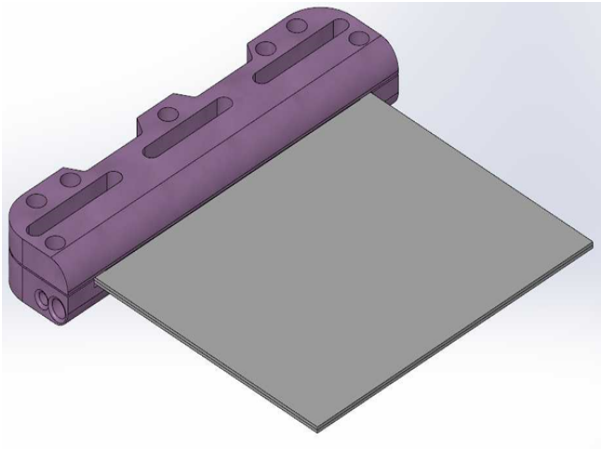

C

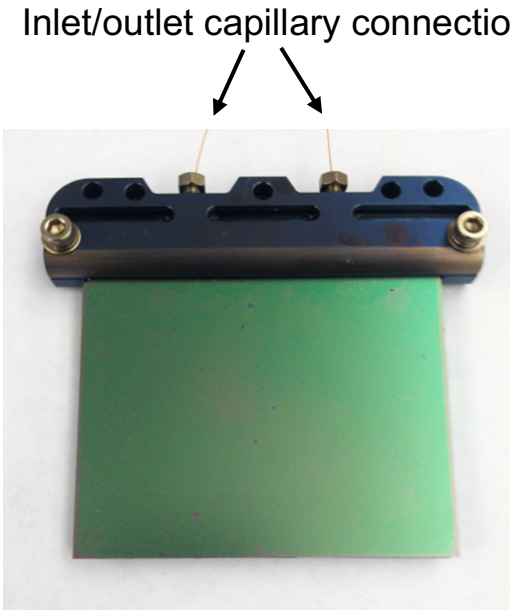

Figure 3 A, B, C

A

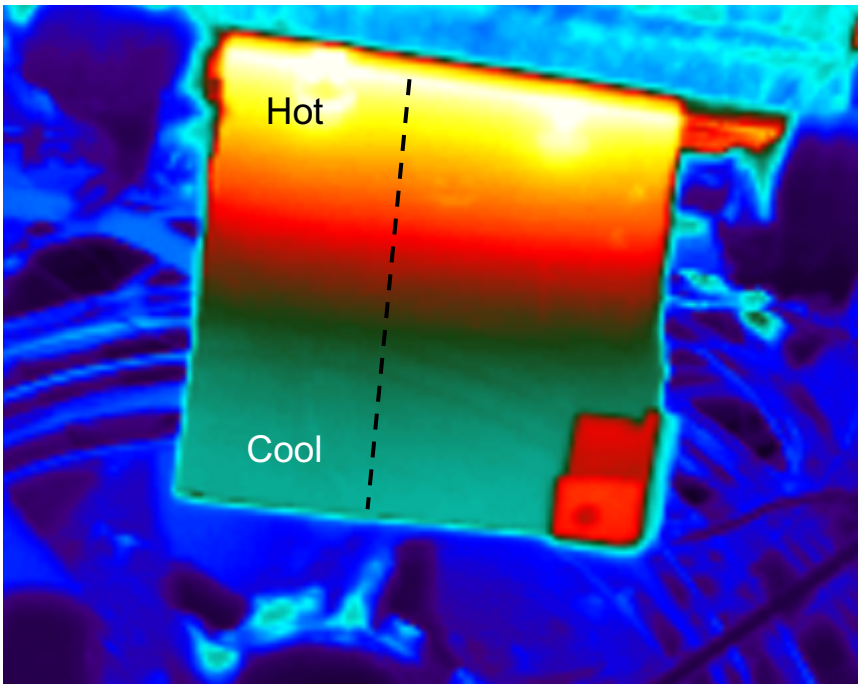

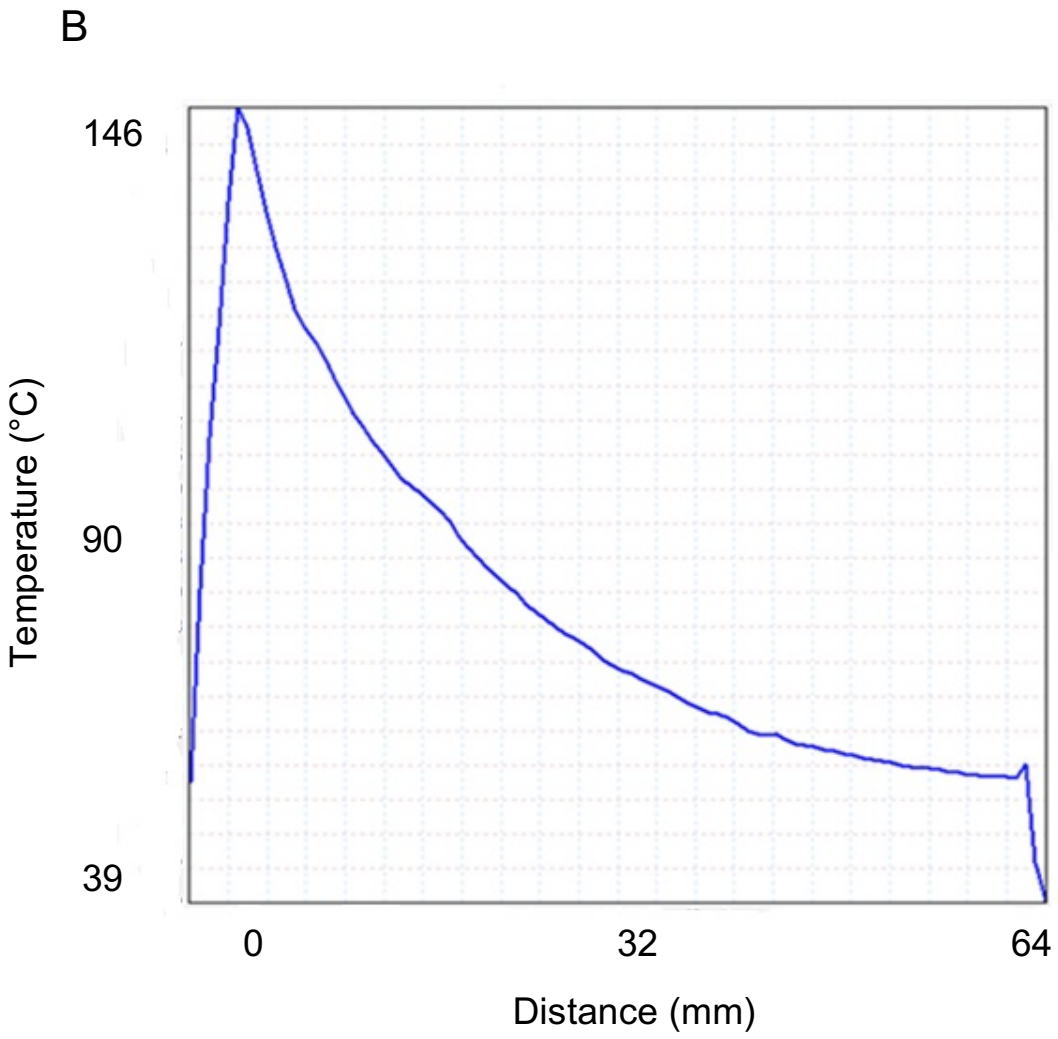
B
146
90
39
Temperature (°C)
0
32
64
Distance (mm)

C

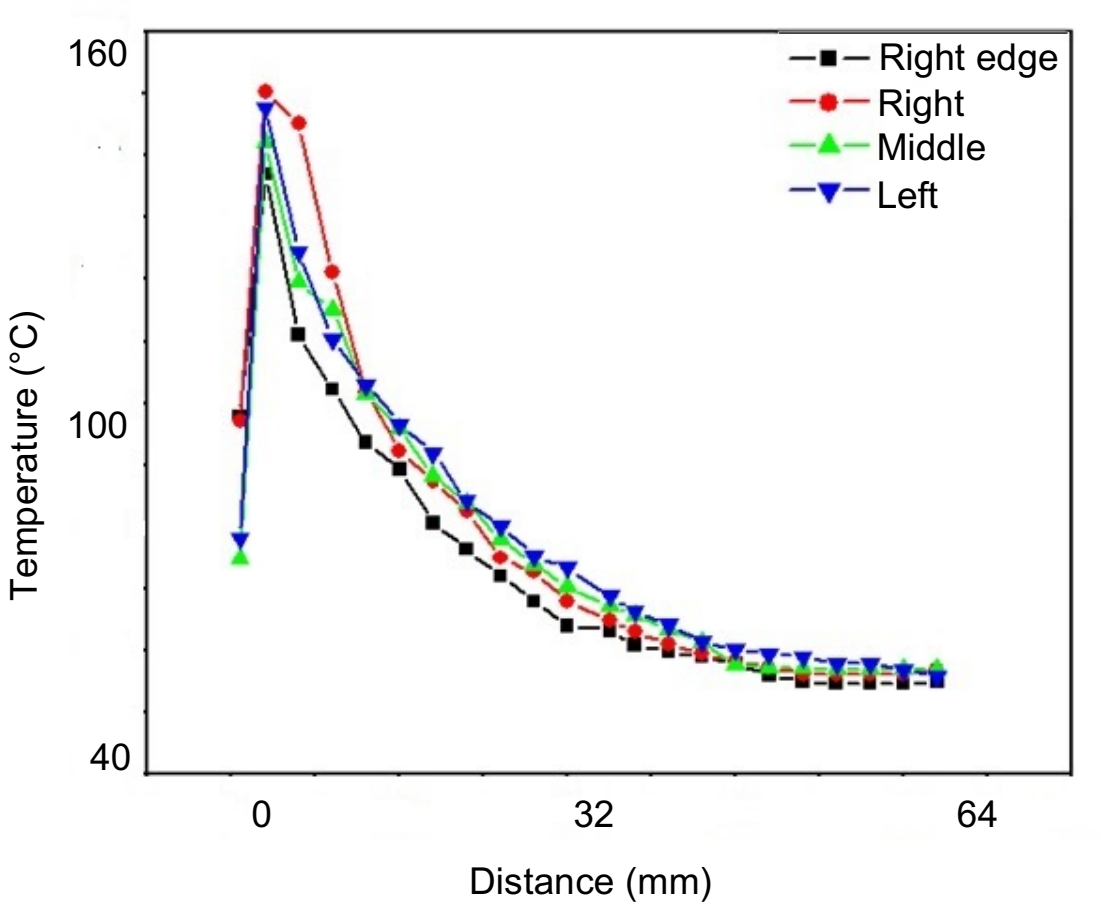
160
100
40
Temperature (°C)
0
32
64
Distance (mm)
Right edge
Right
Middle
Left

Figure 4

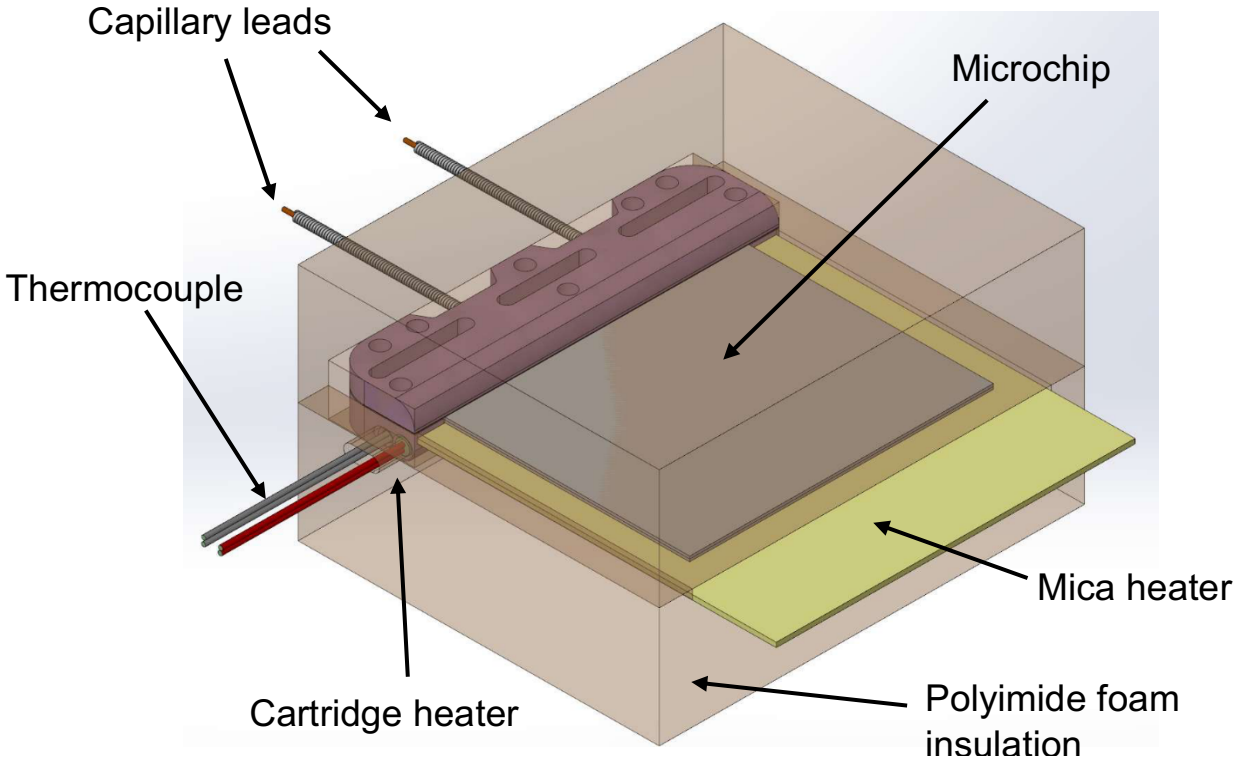
Capillary leads
Microchip
Thermocouple
Mica heater
Cartridge heater
Polyimide foam
insulation

Figure 5

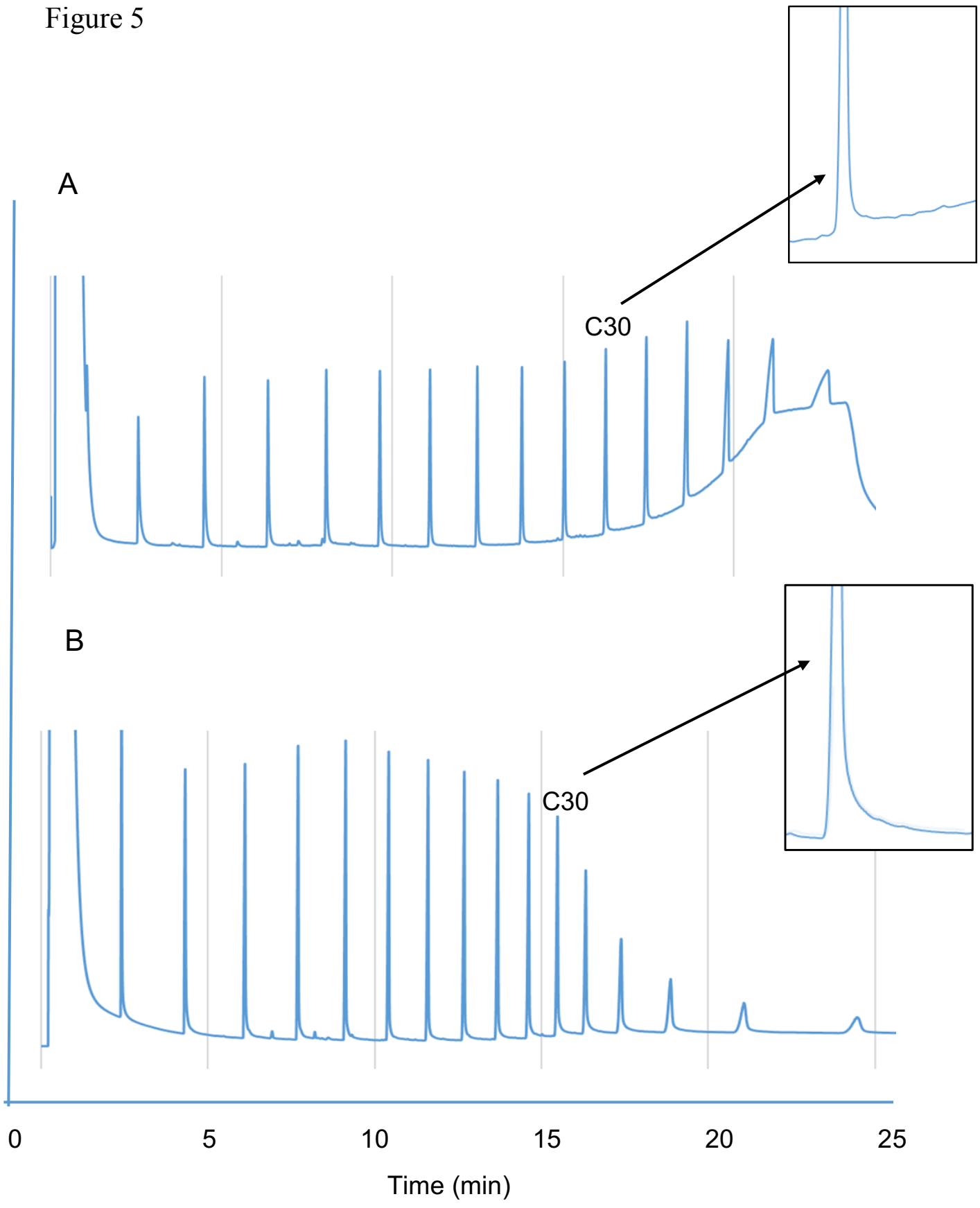

Figure 6

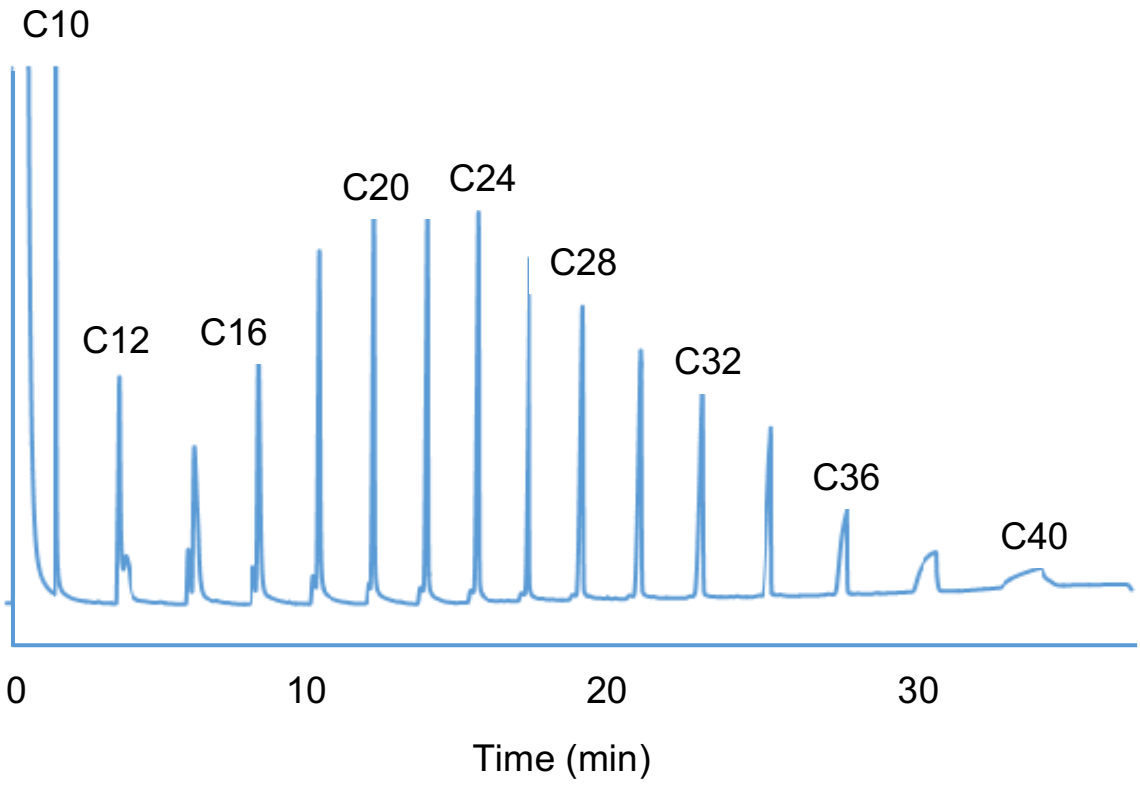

Figure 7

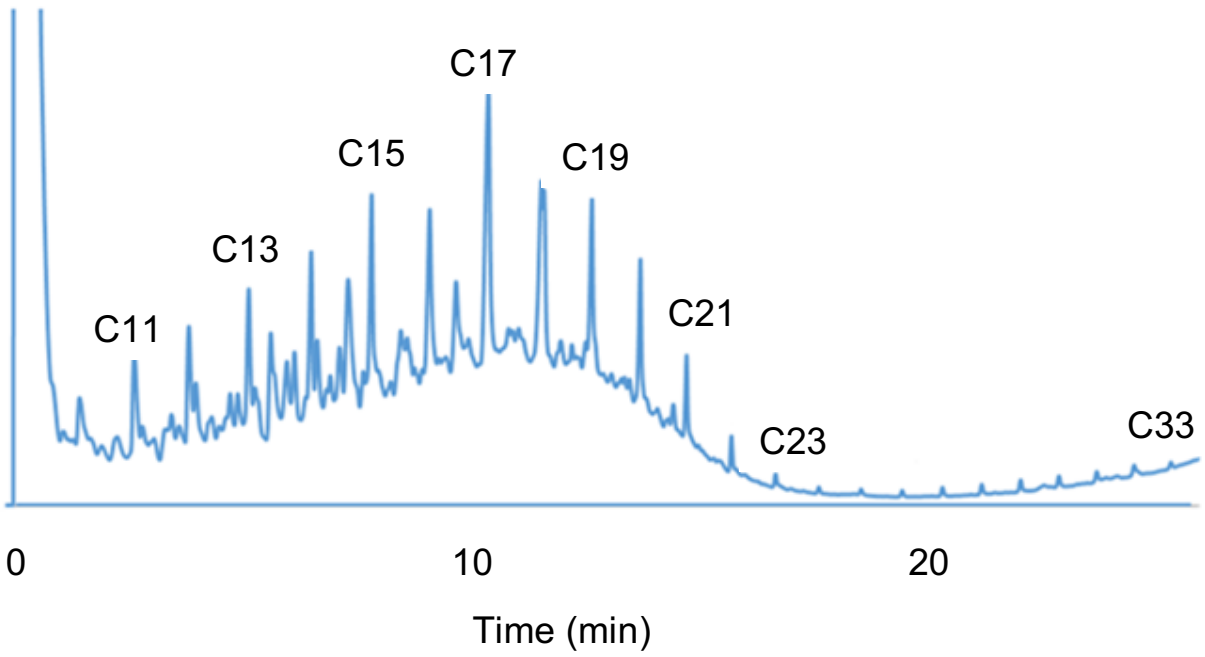

Figure 8